Target patterns arising from the short-wave instability in near-critical regimes of reaction-diffusion systems

Arkady B. Rovinsky,* Anatol M. Zhabotinsky,† and Irving R. Epstein‡
Department of Chemistry and Volen Center for Complex Systems, Brandeis University, Waltham, Massachusetts 02254-9110
(Received 25 September 1996; revised manuscript received 4 February 1997)

The supercritical short-wave oscillatory bifurcation is studied in finite systems using the amplitude (Ginzburg-Landau) equation. Numerical simulations show that a zero-flux boundary stabilizes sources of target patterns. As a result, stable sources attached to the boundary can exist at small overcriticality, under the condition of convective instability of the homogeneous steady state. Oscillating target patterns and alternating wave packets are formed if the coupling between left and right propagating waves is strong. [S1063-651X(97)01807-2]

PACS number(s): 03.40.Kf, 82.20.Mj, 42.25.Gy

I. INTRODUCTION

In extended systems, three types of simple instabilities of a spatially uniform steady state are responsible for a variety of patterns which can be classified as follows: (1) oscillatory in time and uniform in space, (2) stationary in time and periodic in space, and (3) oscillatory in space and time [1]. For reaction-diffusion systems, all three instabilities were studied by Turing [2]. Of these three, the oscillatory instability at finite wave number, i.e., the short-wave instability, is the least studied.

The short-wave instability has been found in binary fluid convection and in electroconvection in liquid crystals [1]. Recently, standing waves and other spatiotemporal patterns connected with this type of instability have been found in oscillating heterogeneous reactions when diffusion of the autocatalyst (activator) is supplemented by a global negative feedback. Jakubith *et al.* [3] found standing concentration waves in carbon monoxide oxidation on the surface of a Pt monocrystal. These standing waves were obtained in a mathematical model that took into account the surface reactions, surface diffusion of the autocatalyst, and global coupling through the gas phase [4]. Standing waves were observed during electrochemical dissolution of nickel [5], and various relevant patterns were found during the atmospheric oxidation of hydrogen, propylene, methylamine, and ammonia on heated metallic wires and ribbons [6]. Middya *et al.* performed systematic simulations with simple models of relaxation oscillators supplemented with diffusion and global negative feedback. They found various types of standing waves, target patterns, and some more complicated patterns [7].

Recently, a simple reaction-diffusion model has been developed that contains a relatively large domain of the wave instability. One-dimensional simulations show that the model can generate traveling and standing waves, modulated waves, alternating waves on rings, asymmetric standing-traveling wave patterns, and target patterns, as well as fusion and splitting of defects [8].

Target patterns seem to be the most important of the patterns that can be generated by the short-wave instability in reaction-diffusion systems, because spontaneous desynchronization of bulk oscillations in real reaction-diffusion systems usually begins with the emergence of target patterns [9–11]. While in experiments target patterns often arise from local inhomogeneities in system parameters [12–14] (e.g., from dust particles or impurities that locally change reaction rates), there is a good deal of evidence that these patterns can also emerge from fluctuations of the concentrations that are dynamic variables of the system [11,15].

The target patterns found in the above models emerge rather far from the onset of the short-wave instability. To find general conditions for a generation of target patterns near the onset, one can analyze the corresponding amplitude, i.e., the complex Ginzburg-Landau, equations (GLE).

$$\dot{A} = \epsilon A - a|A|^2 A - b|B|^2 A - v A_x + d A_{xx}, \tag{1}$$

$$\dot{B} = \epsilon B - a|B|^2 B - b|A|^2 B + v B_x + d B_{xx}, \tag{2}$$

where A is the complex amplitude of the mode traveling to the right, B is that of the mode traveling to the left, and ϵ is the overcriticality parameter; v is the group velocity, which is a real number.

Target pattern formation in coupled complex GLE has been studied by several authors [16–22]. However, these studies do not consider the effects of boundary conditions, which are significant in experimental reaction-diffusion systems. Livshits [16] and Coullet and co-workers [17,21] considered a spatially infinite system, so that boundary effects were irrelevant. In the context of reaction-diffusion systems, their results imply that stable target patterns can only exist for large overcriticality ($\epsilon > v^2 \mathrm{Re}(d)/4|d|^2$, which is the condition of absolute instability [23]), when the validity of the Ginzburg-Landau description has not been rigorously

*Electronic address: rovinsky@ep2.chem.brandeis.edu
†Electronic address: zhabotinsky@binah.cc.brandeis.edu
‡Electronic address: epstein2@binah.cc.brandeis.edu

proved. Cross [18–20] performed an extensive computer study of the GLE with real coefficients in finite systems with no-slip boundary conditions. While these calculations are relevant to convection problems, a similar approach to reaction-diffusion systems normally involves complex GLE with zero-flux boundary conditions. Therefore, the problem of whether the short-wave instability can underlie the mechanism of target patterns in reaction-diffusion systems still exists.

Here we perform a numerical study of the oscillatory Turing bifurcation in the Ginzburg-Landau approximation without restrictions on the coefficients of the corresponding generalized GLE. Systems with periodic and zero-flux boundary conditions are considered. In this approximation, it is these conditions—the absence of bulk flow and of matter exchange through the walls—that correspond to specific features of the original reaction-diffusion systems. We show that, within a certain range of the mode coupling parameter, stable stationary sources of target patterns can exist in the system at small overcriticalities if they are attached to zero-flux boundaries. These structures become oscillating when the coupling between the left-going and right-going waves increases. With still stronger coupling, this oscillation may evolve into a regime of alternating wave packets emitted by the opposite boundaries. In contrast, free-standing sources are only found at a sufficiently large overcriticality, when the instability of the uniform steady state is absolute, in agreement with the argument of Coullet, Frisch, and Plaza [21] for infinite systems.

In Sec. II we discuss GLE for short-wave bifurcation. Section III describes the numerical procedure employed for the simulations. Sections IV and V treat the cases of periodic boundary conditions and zero-flux boundary conditions, respectively. After Sec. VI, the Appendix gives a derivation of boundary conditions for the GLE corresponding to zero-flux boundary conditions for the original reaction-diffusion system.

II. SCALING GINZBURG-LANDAU EQUATION FOR THE OSCILLATORY TURING BIFURCATION

Here we make Eqs. (1) and (2) dimensionless by using scales different from that of [1,16–19]. In the generic case $v=O(k_{cr}D)$, where k_{cr} is the wave number of the critical mode, and D is a ''characteristic'' diffusion coefficient. Both $\mathrm{Re}(d)$ and $\mathrm{Im}(d)=O(D)$ After the rescaling: $t\mapsto t/\epsilon$, $A\mapsto[\epsilon/\mathrm{Re}(a)]^{1/2}A$, $B\mapsto[\epsilon/\mathrm{Re}(a)]^{1/2}B$, $x\mapsto(v/\epsilon)x$, Eqs. (1) and (2) become

$$\dot{A}=A-(1+i\alpha)|A|^2A-\gamma(1+i\beta)|B|^2A-A_x+\delta(1+i\delta')A_{xx}\,, \tag{3}$$

$$\dot{B}=B-(1+i\alpha)|B|^2B-\gamma(1+i\beta)|A|^2B+B_x+\delta(1+i\delta')B_{xx}\,, \tag{4}$$

where $\alpha=\mathrm{Im}(a)/\mathrm{Re}(a)$, $\gamma=\mathrm{Re}(b)/\mathrm{Re}(a)$, $\beta=\mathrm{Im}(b)/\mathrm{Re}(b)$, $\delta'=\mathrm{Im}(d)/\mathrm{Re}(d)$, and $\delta=\epsilon\,\mathrm{Re}(d)/v^2$. Note that $\delta=O(\epsilon/k_{cr}^2D)$, and in the generic case $k_{cr}^2D=O(1)$. Thus $\delta=O(\epsilon)$, and we treat it as an overcriticality parameter.

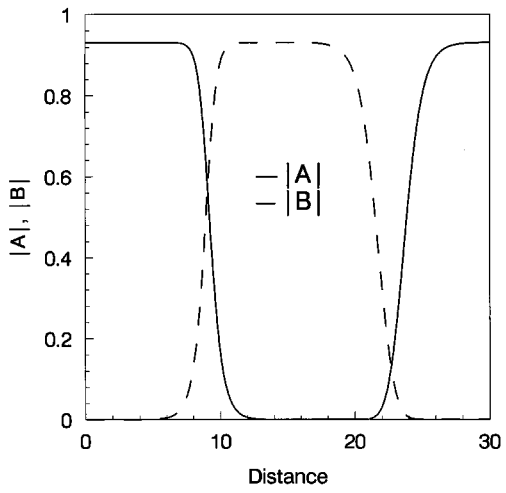

FIG. 1. A stationary target pattern in a system with periodic boundary conditions. The solid line is the stationary envelope of the amplitude of the rightward traveling wave, and the dashed line is that of the wave traveling leftward. The crossover at distance ≈ 10 is a sink and that at ≈ 23 is a source. Parameters: $\alpha=0.5$, $\beta=0.25$, $\delta'=0.5$, $\gamma=4$, and $\delta=0.2$. The units of both axes are dimensionless.

In an infinite, or periodic, system two types of solutions are known: standing waves (if $-1<\gamma<1$), and traveling waves (if $\gamma>1$). Since sources of traveling waves are the focus of the present work, we perform simulations of Eqs. (3) and (4) for $\gamma>1$, outside the domain of the Benjamin-Feir instability [24] $(1+\alpha\delta'>0)$.

III. NUMERICAL PROCEDURES

Since the complex ODEs (3) and (4) represent an ideally ''soft'' system (having only one time scale), the stability requirements for the numerical integration are not very restrictive. Therefore, the equations were integrated with the first order Euler technique. Double precision complex arithmetic was used. The time and space discretizations were chosen such that their further refinement did not improve the results significantly. The time step was varied within the interval $1–5\times10^{-4}$ and the number of spatial grid points varied from 400 to 800. Two kinds of initial conditions were used: (a) $A=0.005[1+iR_1(x)]$, $B=0.09[1+iR_2(x)]$ for $x<x_0$, and $A=0.1[1+iR_1(x)]$, $B=0.001[1+iR_2(x)]$ for $x>x_0$, where R_j is a random number normally distributed in the interval (0,1); x_0 is the initial position of the source; (b) $A=0.1[R_1(x)+iR_2(x)]$, $B=0.1[R_3(x)+iR_4(x)]$, $0<x<L$. The (b) type initial conditions were only used for systems of length $L\leqslant 10$, where no free-standing sources were found.

IV. PERIODIC BOUNDARY CONDITIONS

For $\delta<\delta_{cr}$ ($\delta_{cr}=0.2$ for our parameters) the solution always converges to a homogeneous traveling wave. Stationary target patterns exist if $\delta\geqslant\delta_{cr}$ and the system is long enough (Fig. 1). Figure 2 shows the domain of target patterns

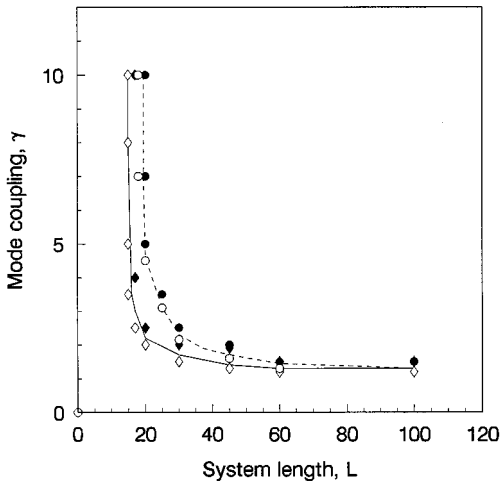

FIG. 2. The domain of stationary target patterns in a system with periodic boundary conditions. Solid line and diamonds: $\delta=0.25$, dashed line and circles: $\delta=0.2$. Other parameters are as in Fig. 1.

in the γ-L plane for the case of a single target pattern (a ''source'' and a ''sink'') present in the system. This figure suggests the existence of a critical length above which the system can support free-standing pacemakers. More than one stable target pattern can be found in a sufficiently long system (Fig. 3).

V. ZERO-FLUX BOUNDARY CONDITIONS

Zero-flux boundary conditions imply reflection symmetry with respect to the boundary. Stationary sources and sinks also possess reflection symmetry. Therefore, if a system with a stationary source and/or sink is cut in two at the point of reflection symmetry and the zero-flux condition is imposed at the new edge, the new ''half'' of the system should still admit the corresponding half of the originally symmetric solution. Hence, if a source or sink can exist within a system, it should also exist at the zero-flux boundary. However, zero-flux boundary conditions impose the reflection symmetry constraint not only on the solutions but on possible perturbations as well. Therefore, solutions in a system with zero-flux boundaries are subject to a narrower class of possible perturbations, in comparison with those in infinite or periodic systems, and their stability domain may expand as a result. For this reason, one can anticipate stability of sources attached to a zero-flux wall even for $\delta<\delta_{cr}$. Our simulations described below confirm this conjecture.

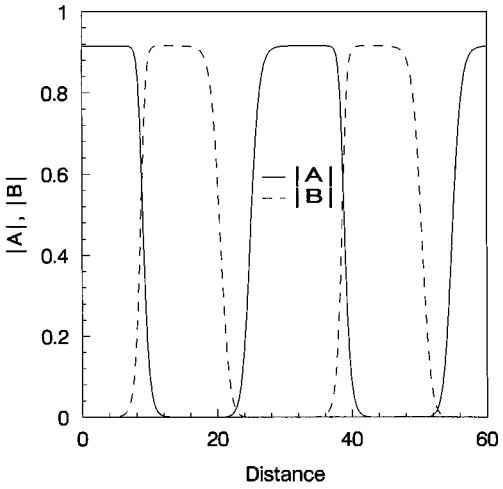

FIG. 3. Two stationary target patterns in a longer system with periodic boundary conditions. Parameters are as in Fig. 1.

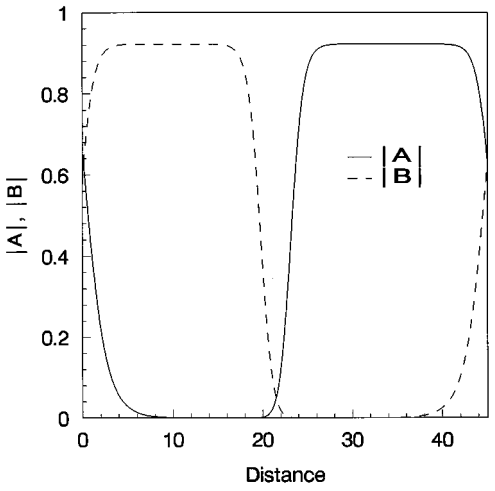

FIG. 4. A stationary target pattern in a system with zero-flux boundary conditions. Parameters: $\alpha=0.5$, $\beta=0.25$, $\gamma=2.0$, $\delta'=0.5$, $\delta=0.2$. The units of both axes are dimensionless.

The original zero-flux boundary conditions for the reaction-diffusion equations result in the following boundary conditions for the coupled GLE (see the Appendix):

$$[\partial_x A(x,t)+\partial_x B(x,t)]_{x=0,L}=0, \tag{5}$$

$$[A(x,t)-B(x,t)]_{x=0,L}=0. \tag{6}$$

As in the case of periodic boundary conditions, stationary free-standing sources can be found in a sufficiently long system (Fig. 4) for $d_0\geqslant\delta_{cr}$. The domain of their existence (Fig. 5) differs insignificantly from that found in the preceding section. Even in a long system, a free-standing source can be stable only far enough from the boundary: otherwise it drifts and eventually attaches to the boundary (Fig. 6). For shorter systems ($L\leqslant 15$ in our simulations) the sources and sinks can only exist if they are attached to the boundaries. Figure 7 illustrates a typical solution when calculations start from spatially asymmetric (e.g., random) initial conditions.

While we have found stationary free-standing sources only under the conditions of absolute instability $\delta\geqslant\delta_{cr}$, stable sources at the boundaries can exist for small δ (i.e., for small overcriticality and under the condition of convective instability) if the coupling parameter γ is in the range 1–1.6, see Fig. 8. In a short system ($L\sim 10$) a target pattern extends over the entire system, with the source attached to one boundary and the sink attached to the other. In a longer system, each boundary may become a source, with the sink settling in between (Fig. 9). These results imply that a zero-flux boundary, such as a wall or a dust particle, may become a source even at a very small overcriticality.

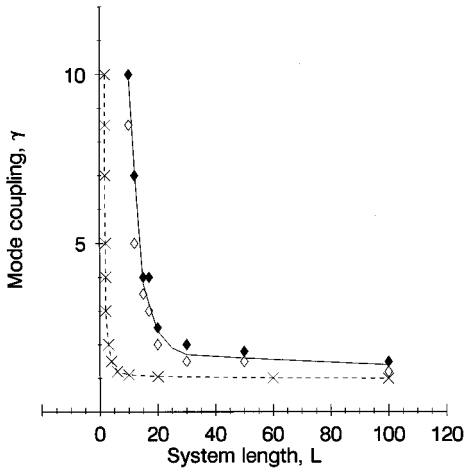

FIG. 5. The domain of stationary free-standing target patterns in a system with zero-flux boundary conditions is above the solid line. The region between the solid and dashed lines is the domain of stationary sources attached to the boundary. There are no sources below the dashed line. Parameters are as in Fig. 4.

When γ exceeds a certain threshold ($\gamma > \gamma_0 \approx 1.7$ in our case) and $\delta < \delta_{cr}$, sources at the boundaries become oscillatory (Figs. 8 and 10). For small δ and large enough γ the solution takes a form of alternating wave packets, see Fig. 11.

VI. DISCUSSION

As mentioned, Eqs. (3) and (4) have been considered in a number of works [16–22]. However, in Ref. [16] the diffusion term was completely neglected, while in Refs. [17–22] it was taken to be of the same order of magnitude as the other terms. Moreover, in the fluid dynamics context, the numerical simulations in Ref. [18–20] were performed with the real valued equations. Each of these cases would correspond to some type of degeneracy when taken in the context of reaction-diffusion systems.

We consider here Eqs. (3) and (4) without these restrictions. For this reason, to obtain Eq. (2) we employ a spatial scaling different from that used in Refs. [1,17–21]: we use the ''convective length'' $l_c = v/\epsilon$ as a scaling parameter instead of the ''diffusion length'' $l_d = [\mathrm{Re}(d)/\epsilon]^{1/2}$. While both scales are of the same order of magnitude in the above references, since vanishing group velocities are considered in the context of the fluid convection problem $v = O(\epsilon^{1/2})$, only the ''convective length'' is justified at finite group velocities, which is the generic case in reaction-diffusion systems.

Solutions that correspond to one-dimensional target patterns are of special interest here. We have shown that a zero-flux boundary may be a source of target patterns at very small overcriticality. While it was previously thought that an inhomogeneity may become a nucleus of a target pattern if it

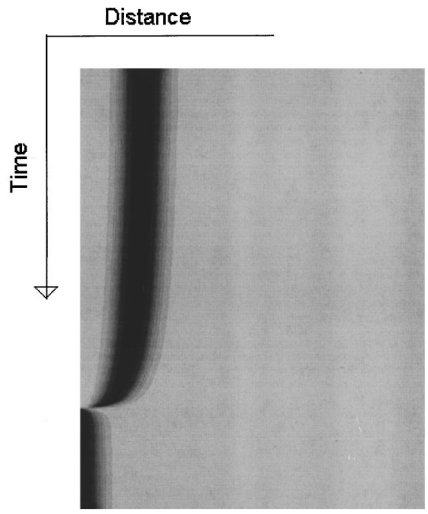

FIG. 6. Drift of a source toward a boundary when its initial distance from the boundary is 1/5 of the system length. Sources located at a distance $> L/3$ from the boundaries remain stable in this case. The gray levels represent the value of $|A| + |B|$, with the dark corresponding to a low value, and the light to a high value. Parameters are as in Fig. 4 except for $L = 50$.

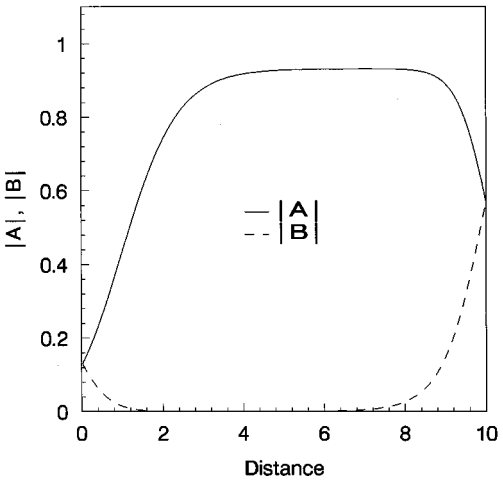

FIG. 7. A stable source and a sink attached to the zero-flux boundaries. Parameters are as in Fig. 4, except for $\delta = 0.3$ and $\gamma = 4$.

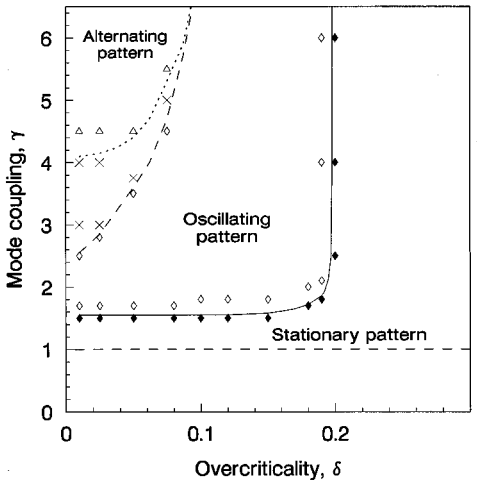

FIG. 8. The domains of stationary, oscillating, and alternating sources attached to the boundary. The area between the dashed and dotted lines is a domain of complex alternating patterns. Parameters are as in Fig. 4, $L = 10$.

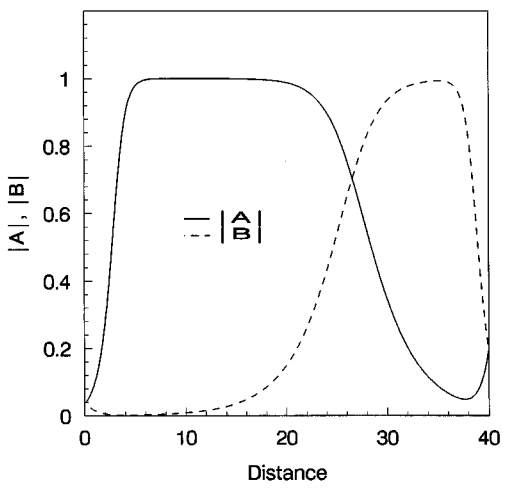

FIG. 9. Stationary sources attached to zero-flux boundaries for $\delta < \delta_{cr}$. Parameters: $\alpha = 0.5$, $\beta = 0.25$, $\gamma = 1.3$, $\delta' = 0.5$, and $\delta = 0.05$.

appropriately changes the local kinetic parameters of the system [12–14], our work shows that ''neutral'' walls or dust particles may also be pacemakers in the case of the oscillatory Turing bifurcation in a reaction-diffusion system.

ACKNOWLEDGMENTS

We gratefully acknowledge the support of the National Science Foundation Chemistry Division and the W.M. Keck Foundation.

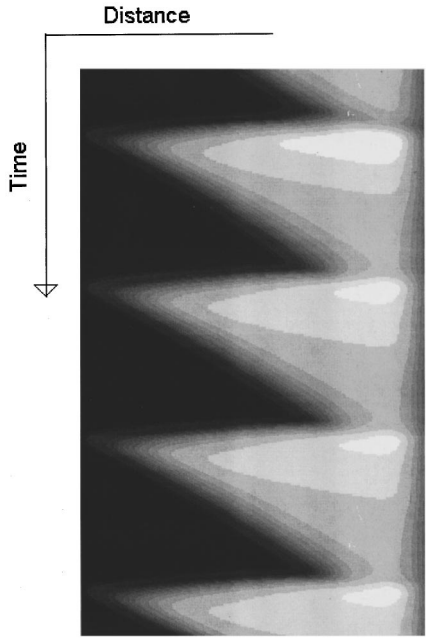

FIG. 10. An oscillating source in a system with zero-flux boundaries. The gray level represent the value of $|A|$, i.e., the amplitude of the wave traveling to the right, with the dark corresponding to a low value, and the light to a high value. Parameters are as in Fig. 4, except for $\delta = 0.1$ and $L = 10$.

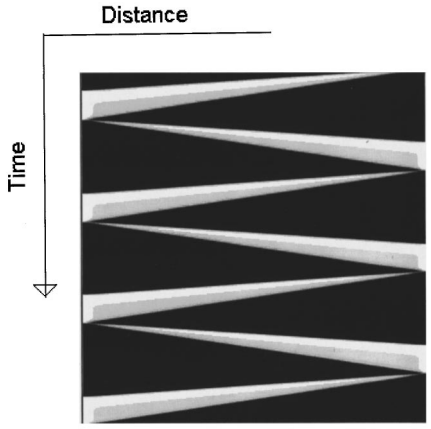

FIG. 11. Alternating wave packets in a system with zero-flux boundaries. The gray levels represent the value of $|A|+|B|$, i.e., the amplitudes of the waves traveling to the right and to the left, with the dark corresponding to a low value, and the light to a high value. In these calculations when one of the amplitudes was high, the other was near zero. Parameters are as in Fig. 4, except for $\delta = 0.005$, $\gamma = 10$, and $L = 10$.

APPENDIX

To obtain the boundary conditions for the complex amplitudes A and B one has to recall how these amplitude relate to the solutions of the original reaction-diffusion system. Consider the reaction-diffusion system

$$\dot{\mathbf{X}} = \mathbf{f}(\mathbf{X}) + \mathbf{D}\Delta\mathbf{X}, \tag{A1}$$

and suppose that it has a homogeneous solution $\mathbf{X} = \mathbf{X_0}$. Linearization of Eq. (A1) near $\mathbf{X_0}$ yields

$$\dot{\mathbf{x}} = \mathbf{A}\mathbf{x} + \mathbf{D}\Delta\mathbf{x}, \tag{A2}$$

where $\mathbf{x} = \mathbf{X} - \mathbf{X}_0$, $\mathbf{f}(\mathbf{X}_0) = 0$, and $\mathbf{A}_0 = (\partial\mathbf{f}/\partial\mathbf{x})_{\mathbf{X}=\mathbf{X_0}}$ is the Jacobian matrix. We also assume that there is a critical wave number k_{cr}, such that for $\mathbf{x} = \mathbf{x}_{k_{cr}} \exp(ik_{cr}r)$ there is a pair, $\lambda_{1,2} = \pm i\omega$, of purely imaginary eigenvalues of the matrix $\mathbf{A} = \mathbf{A}_0 - k_{cr}^2\mathbf{D}$, while for $k \neq k_{cr}$ all the real parts of eigenvalues are negative. Then the inhomogeneous solution is sought in the form

$$\begin{aligned}\mathbf{x} = {} & A(r,t)\exp[i(\omega t - k_{cr}r)]\mathbf{U} + B(r,t) \\ & \times \exp[i(\omega t + k_{cr}r)]\mathbf{U} + \overline{A}(r,t) \\ & \times \exp[-i(\omega t - k_{cr}r)]\overline{\mathbf{U}} + \overline{B}(r,t) \\ & \times \exp[-i(\omega t + k_{cr}r)]\overline{\mathbf{U}},\end{aligned} \tag{A3}$$

where $\mathbf{U}$ is the right eigenvector of $\mathbf{A}$ corresponding to $\lambda = i\omega$, and $A(r,t)$ and $B(r,t)$ are the slowly varying amplitudes described by Eqs. (3) and (4). The zero-flux boundary condition $(\partial\mathbf{x}/\partial r)_{r=0} = 0$ then reduces to

$$0 = \left[\frac{\partial A(0,t)}{\partial r} - ik_{cr}A(0,t) + \frac{\partial B(0,t)}{\partial r} + ik_{cr}B(0,t)\right] \times \exp(i\omega t)\mathbf{U} + \left[\frac{\partial \overline{A}(0,t)}{\partial r} - ik_{cr}\overline{A}(0,t)\right.$$

$$+\frac{\partial \overline{B}(0,t)}{\partial r}+ik_{cr}\overline{B}(0,t)\Bigg]\exp(-i\omega t)\overline{\mathbf{U}}, \tag{A4}$$

which, after multiplying from the left by the left eigenvector $\mathbf{U}^{+}$, becomes

$$\frac{\partial A(0,t)}{\partial r}+\frac{\partial B(0,t)}{\partial r}-ik_{cr}[A(0,t)-B(0,t)]=0. \tag{A5}$$

The fact that $A(r,t)$ and $B(r,t)$ are slowly varying functions of the spatial variable can be expressed as $A=A(\epsilon^{1/2}r,t)$, $B=B(\epsilon^{1/2}r,t)$. Then Eq. (A5) turns into

$$\epsilon^{1/2}[\partial_{\xi}A(0,t)+\partial_{\xi}B(0,t)]-ik_{cr}[A(0,t)-B(0,t)]=0, \tag{A6}$$

where $\xi=\epsilon^{1/2}r$. The requirement that the terms of different order in ϵ should balance separately finally yields the boundary conditions for Eqs. (3) and (4)

$$\partial_r A(0,t)+\partial_r B(0,t)=0, \tag{A7}$$

$$A(0,t)-B(0,t)=0. \tag{A8}$$

[1] M.C. Cross and P.C. Hohenberg, Rev. Mod. Phys. **65**, 851 (1993).

[2] A. Turing, Philos. Trans. R. Soc. London, Ser. A **237**, 37 (1952).

[3] S. Jakubith, H. H. Rotermund, W. Engel, A. von Oertzen, and G. Ertl, Phys. Rev. Lett. **65**, 3013 (1990).

[4] H. Levine and X. Zou, Phys. Rev. E **48**, 50 (1993); M. Falcke, H. Engel, and M. Neufeld, *ibid.* **52**, 763 (1995).

[5] O. Lev, M. Sheintuch, L.M. Pismen, and Ch. Yarnitzky, Nature (London) **336**, 458 (1988).

[6] G.A. Cordonier, F. Schuth, and L.D. Schmidt, J. Chem. Phys. **91**, 5374 (1989); G.A. Cordonier and L.D. Schmidt, Chem. Eng. Sci. **44**, 1983 (1989); G. Philippou, F. Schultz, and D. Luss, J. Phys. Chem. **95**, 3224 (1991); D. Graham, S.L. Lane, and D. Luss, *ibid.* **97**, 7564 (1993).

[7] U. Middya, M. D. Graham, D. Luss, and M. Sheintuch, J. Chem. Phys. **98**, 2823 (1993); U. Middya, D. Luss, and M. Sheintuch, *ibid.* **101**, 4688 (1994); U. Middya and D. Luss, *ibid.* **102**, 5029 (1995).

[8] A.M. Zhabotinsky, M. Dolnik, and I.R. Epstein, J. Chem. Phys. **103**, 10306 (1995).

[9] A.N. Zaikin and A.M. Zhabotinsky, Nature (London) **225**, 535 (1970).

[10] A.M. Zhabotinsky and Z.N. Zaikin, J. Theor. Biol. **40**, 45 (1973).

[11] *Oscillations and Traveling Waves in Chemical Systems*, edited by R.J. Field and M. Burger (Wiley, New York, 1985).

[12] J.J. Tyson and P.C. Fife, J. Chem. Phys. **73**, 2224 (1980).

[13] A.T. Winfree, in *Oscillations and Traveling Waves in Chemical Systems*, edited by R.J. Field and M. Burger (Wiley, New York, 1985), p. 441.

[14] K.I. Agladze and V.I. Krinsky, in *Self-Organization. Autowaves and Structures far from Equilibrium*, edited by V.I. Krinsky (Springer, Berlin, 1984), p. 147.

[15] C. Vidal, A. Pagola, J.M. Bodet, P. Hanusse, and E.J. Bastardie, J. Phys. (France) **47**, 1999 (1986); A. Pagola and C. Vidal, J. Chem. Chem. **91**, 501 (1987); C. Vidal, J. Stat. Phys. **48**, 1017 (1987); C. Vidal and A. Pagola, J. Phys. Chem. **93**, 2711 (1989).

[16] M.A. Livshits, Z. Phys. B **53**, 83 (1983).

[17] P. Coullet, S. Fauve, and E. Tirapegui, J. Phys. (France) Lett. **46**, 787 (1985).

[18] M.C. Cross, Phys. Rev. Lett. **57**, 2935 (1986).

[19] M.C. Cross, Phys. Rev. A **38**, 3593 (1988).

[20] M.C. Cross and E.Y. Kuo, Physica D **59**, 90 (1992).

[21] P. Coullet, T. Frisch, and T. Plaza, Physica D **62**, 75 (1993).

[22] B.A. Malomed, Phys. Rev. E **50**, R3310 (1994).

[23] R.J. Deissler, J. Stat. Phys. **40**, 371 (1985).

[24] T.B. Benjamin and J.E. Feir, J. Fluid Mech. **27**, 417 (1967).